

## Substrate for atomic chain electronics

Toshishige Yamada\*

T27A-1, MRJ, NASA Ames Research Center, Moffett Field, California 94035

Charles W. Bauschlicher, Jr. and Harry Partridge

STC-230-3, NASA Ames Research Center, Moffett Field, California 94035

(Received 2 September 1998; revised manuscript received 9 February 1999)

A substrate for future atomic chain electronics, where adatoms are placed at designated positions and form atomically precise device components, is studied theoretically. Since the van der Waals force turns out inappropriately weak, adatoms have to be secured with chemical bonding to the substrate atoms, but then electronic isolation between the adatom and substrate systems is not always guaranteed. A chain model shows that good isolation is expected on an *s-p* crossing substrate such as Si, Ge, or GaAs through surface localization, reflecting the *bulk* nature of the substrate. Isolation is better if adatoms are electronically similar to the substrate atoms, and can be manipulated by hydrogenation. Chain structures with group IV adatoms with two chemical bonds, or group III adatoms with one chemical bond, are semiconducting, reflecting the *surface* nature of the substrate. These structures are unintentionally doped due to the charge transfer across the chemical bonds. Physical properties of adatom chains have to be considered for the unified adatom and substrate systems. [S0163-1829(99)00223-4]

### I. INTRODUCTION

When the semiconductor device size is reduced to  $0.07 \mu\text{m}$ , the number of dopant atoms in the channel is no longer macroscopic, typically less than a hundred.<sup>1-3</sup> A spatial distribution of these dopant atoms fluctuates statistically from device to device even though each device is identically designed and fabricated, and this places a serious limitation for integration. It may be possible to control dopant positions to some extent,<sup>3</sup> but an ultimate control with atomic precision might be difficult. One fundamental solution to this problem is to create electronics that are atomically precise, ordered, and preferably simple. Atomic chains, which are precise structures of adatoms created on an atomically regulated surface using atom manipulation technology,<sup>4</sup> are candidates for constituent components in future electronics. All the adatoms will be placed at designated positions on a substrate, and all the device structures are precise, free from any statistical deviations. It was predicted using a tight-binding method with universal parameters<sup>5,6</sup> that Si chains were metallic and Mg chains were semiconducting regardless of the lattice spacing<sup>7</sup> if the influences of the substrate were neglected. A possible doping scheme was also proposed.<sup>8</sup>

The substrate has to serve as a template for mounting the adatoms so that they are confined with a reasonable strength, and yet has to be electronically isolated from the adatom system so that independent adatom structures do not couple. These requirements often conflict. We need to compromise with either excellent electronic isolation but probably poor structural stability by forbidding chemical bonding between adatoms and substrate atoms, or excellent stability but probably poor isolation by allowing chemical bonding. In the former scheme, the only available mechanism to secure adatoms is van der Waals bonding. To evaluate its strength, an *ab initio* study (Appendix A) has been performed for a Mg adatom on the hydrogenated Si (111) surface<sup>9</sup> using a cluster

model in Figs. 1(a) and 1(b). Table I lists the Mg-adatom height from the upper Si plane, the binding energy, and the effective potential barrier for four sites in Fig. 1(b). The potential minimum occurs at site 3, but the barriers at sites 1 and 4 are so low, 0.39 and 0.52 meV, respectively, that the Mg adatom will not be confined satisfactorily even at liquid-helium temperatures. The situation may not improve drastically for other kinds of substrates within this scheme.

Therefore, the chemical bonding scheme needs to be examined. The worst possible scenario is that an adatom wave function penetrates deep into the substrate and independent adatom structures couple, leading to poor electronic isolation. This problem is closely related to surface localization or how the wave function decays into the substrate. We use a chain model and clarify the existence conditions for surface states. H atoms can manipulate the surface states in a complementary manner on two distinct types of substrates. A prescription for semiconducting adatom chains is described with special requirements for the substrate surface.

In Sec. II, the localization and isolation conditions are clarified. In Sec. III, a prescription for semiconducting chains is described and Ge-adatom chains on Si(100) are discussed. The implication of these results for electronics applications is discussed in Sec. IV.

### II. SURFACE LOCALIZATION AND ELECTRONIC ISOLATION

Edge states, zero-dimensional counterparts of higher-dimensional surface states localizing at the vacuum boundary, will be studied using a chain model representing a substrate. Surface states are supported by many atomic planes parallel to the surface as we will see later. Besides the difficulty in multidimensional modeling with many layers, the physics we are interested in is essentially one dimensional and the chain model prevails for a qualitative study. In fact,

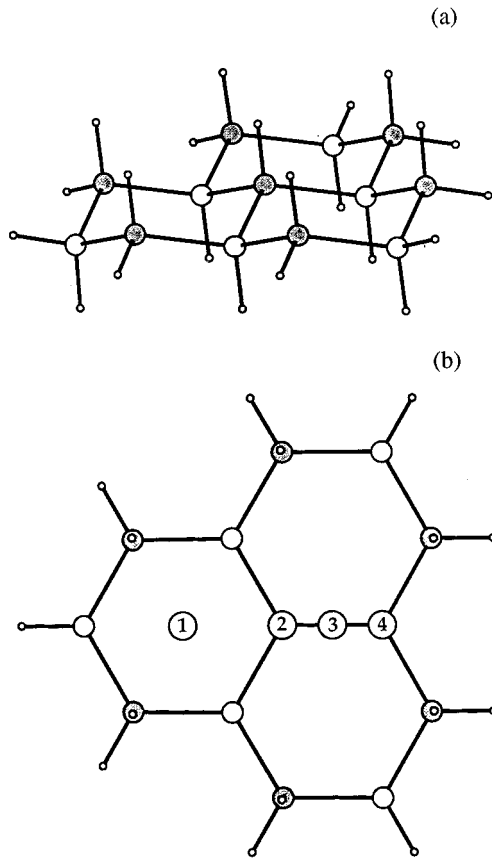


FIG. 1.  $\text{Si}_{13}\text{H}_{22}$  cluster used to model hydrogenated Si (111), where surface Si atoms are shaded: (a) side and (b) top views with four representative sites.

the wave function decays vertically since a reflection from each atomic plane interferes more destructively at a deeper point. This destructive interference is the origin of the surface states, and is one dimensional in nature. In application of the edge-state results to surface states, we can rely on a perturbation picture. When independent, infinitely apart chains are being grouped in bunch to form a finite substrate so that chain edges will form substrate surfaces, the energy levels corresponding to the edge states start widening. Since the bulk valence and conduction bands are widening, the bulk band gap is narrowing. As long as chains are distant, the adatom band widths are narrow and the entire adatom bands are located inside the bulk band gap. In this situation, the existence conditions for the edge states are equivalent to

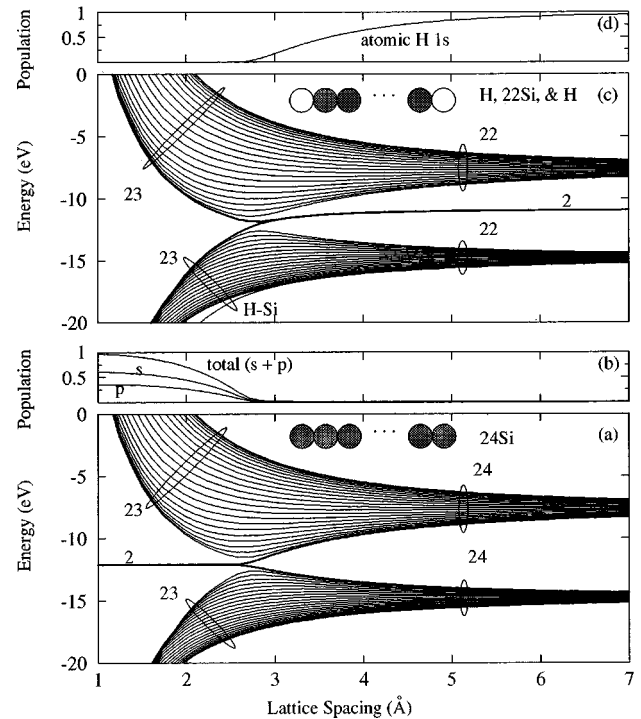


FIG. 2. Electronic states as a function of lattice spacing: (a) energy levels and (b) edge population for states with thick line in 24 Si chain; (c) and (d) the same plots in 22 Si chain with two edge H adatoms.

those for the surface states. When chains are brought closer, the adatom bands may overlap with the bulk bands, but the valence-band maximum and conduction-band minimum that are most important for electronics applications tend to remain inside the bulk band gap. Thus, the tendency of how the edge states behave for various situations will survive in this limit. In the following, energy levels for a finite chain with edge adatoms are calculated as a function of lattice spacing  $d$ . Such plots show how surface states originate from atomic states of constituent atoms as  $d$  is reduced and the crystal is formed.<sup>10-12</sup>

We might think intuitively that unsaturated (dangling-bond) states always localize at the surface, but this is not the case. Figure 2 shows electronic states of a Si atomic chain with an  $s$  orbital and a  $p$  orbital (representing symmetric and antisymmetric bases) as a function of  $d$ , calculated with the tight-binding theory with universal parameters.<sup>5,6</sup> (a) energy levels and (b) edge population for states with thick line in unsaturated chain of 24 Si atoms; (c) and (d) are the same set

TABLE I. Mg adatom height and binding energy for a  $\text{Si}_{13}\text{H}_{22}$  model of hydrogenated Si (111).

Site <sup>a</sup>	Height <sup>b</sup> (Å)	Binding energy <sup>c</sup> (meV)	Effective potential barrier <sup>d</sup> (meV)
1	4.55	57.20	0.39
2	4.86	53.08	4.51
3	4.69	57.59	0.00
4	4.57	57.07	0.52

<sup>a</sup>Sites shown in Fig. 1(b).

<sup>b</sup>Distance from the surface Si-atom plane to the Mg adatom.

<sup>c</sup>Bond functions added midway between the surface H-atom plane and the Mg adatom.

<sup>d</sup>Effective potential barrier measured from site 3.

of plots for a hydrogenated chain of 22 Si atoms. These results are essentially the same if the number of atoms is greater than 16. In both unsaturated and hydrogenated cases, the majority of levels, bulk-penetrating modes, behave similarly. When  $d$  is large, we see  $3s$  and  $3p$  bands in principle. Band widths become wider as  $d$  is reduced. At  $d \sim 2.7 \text{ \AA}$ , both bands meet. This is an  $s$ - $p$  crossing point and the spacing is denoted by  $d_{\text{spc}}$ . For  $d < d_{\text{spc}}$ , a band gap reopens.

In the unsaturated case, edge states appear for  $d < d_{\text{spc}}$  as shown in Fig. 2(b). They are significant mixtures of  $s$  and  $p$  states and there is no apparent correlation for isolated atomic states. There are two edge states, one from the valence band and the other from the conduction band as is obvious by examining the number of states, and they constitute symmetric and antisymmetric modes for the chain center. Twenty-four states will be filled if all the atoms, including adatoms, are assumed to create two chemical bonds to the neighboring chains, and thus the edge states are half filled. Since the filling can be changed by changing the number of adatom chemical bonds, we can eventually design metallic or semiconducting structures using this property as will be discussed in Sec. III.

In the hydrogenated case, edge states appear for  $d > d_{\text{spc}}$ . They are mostly  $s$ -like as in Fig. 2(d), and are identified as isolated  $1s$  states in H. For  $d < d_{\text{spc}}$ , edge states disappear. Thus, the edge states in the hydrogenated case behave in a complementary manner to those in the unsaturated case. Counting an electron from each H atom, 23 states are filled, and edge states are again half filled if the substrate atoms create two chemical bonds to the neighboring chains.

The physical mechanism for this complementary behavior can be intuitively understood as follows. Figure 3 schematically shows the envelope of a wave function  $\phi$  at the vacuum boundary. For  $d < d_{\text{spc}}$  in the unsaturated case,  $\phi$  can connect smoothly into the vacuum and there exist edge states. A H atom provides a symmetric  $1s$ -like wave function (no  $p$  orbitals involved) in the cell, and flips  $d\phi/dx$  without changing the value  $\phi$  at the vacuum boundary. Therefore, once hydrogenated,  $\phi$  cannot connect smoothly without having a notch, and edge states are eliminated. For  $d > d_{\text{spc}}$  in the unsaturated case,  $\phi$  has a notch and edge states are forbidden. When hydrogenated, the smooth connection is now possible because of the flip of  $d\phi/dx$ , and edge states appear.

When a crystal has a natural  $d$  such that  $d < d_{\text{spc}}$ , it is called  $s$ - $p$  crossing, and when  $d > d_{\text{spc}}$ ,  $s$ - $p$  uncrossing. Examples of  $s$ - $p$  crossing crystals are semiconductors such as Si, Ge, or GaAs and many metals, and those of  $s$ - $p$  uncrossing crystals are alkali halides, such as LiF or KCl.<sup>11</sup> Practically, semiconductor substrates may be better since they are widely used in the current device technologies, and are  $s$ - $p$  crossing, supporting surface states at dangling bonds.

Edge states are quite robust. In his original work,<sup>11</sup> Shockley assumed geometrical symmetry for the chain center, but it turns out that this assumption is not essential for the existence of edge states as he had predicted. In order to see it, we have studied an unsaturated chain of 23 Si atoms, where short and long spacings repeat alternately and the chain is nontrivially asymmetric for the central 12th atom. This kind of situation is not rare practically; e.g., Si (111) planes align with alternating spacings of 1 and 3. Due to the

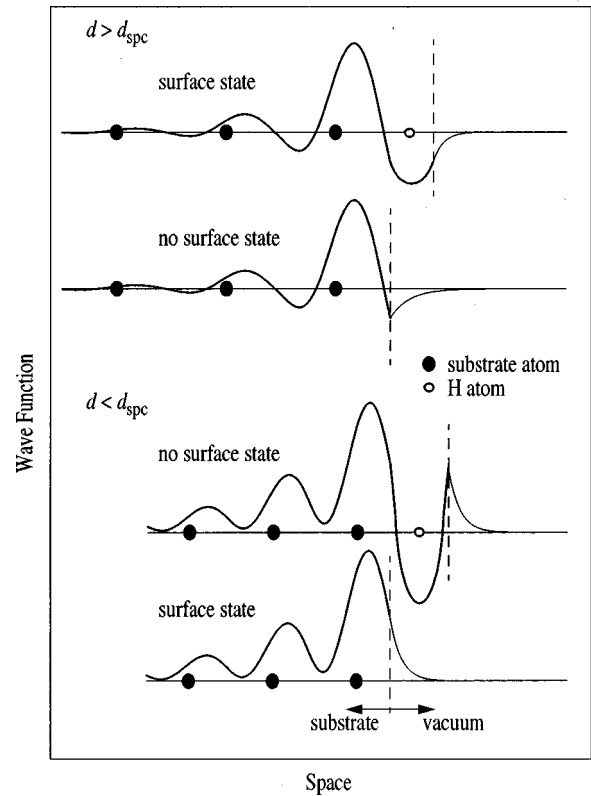


FIG. 3. Schematic plots of wave functions for unsaturated and hydrogenated cases at the vacuum boundary for  $d < d_{\text{spc}}$  (lower two) and  $d > d_{\text{spc}}$  (upper two).

real-space pairing of atoms, the valence and conduction bands split into two, respectively, but edge states still appear in the main band gap for  $d < d_{\text{spc}}$ , in the same way as they do in the symmetric cases.

Different adatoms having both  $s$  and  $p$  orbitals (thus excluding H) can also create edge states for  $d < d_{\text{spc}}$ , but localization is not as good as that for identical adatoms. Figure 4 shows (a) energy levels and (b) edge population for states with thick line in a Si chain with Ge adatoms, and (c) and (d) are the same set of plots with Ga adatoms. Ge is electronically similar to Si in that Ge relevant  $s$  and  $p$  levels are very close to those counterparts in Si, but Ga is not. Ge edge states appear essentially the same way as the unsaturated Si case in Fig. 2(a) for  $d < d_{\text{spc}}$ , while Ga edge states do not appear for  $2.3 \text{ \AA} < d < 2.7 \text{ \AA}$ , due to an overlap in energy with the conduction band. For  $d < 2.3 \text{ \AA}$ , there appear usual  $s$ - $p$  mixed edge states in the band gap. Thus, localization is better for electronically similar adatoms for  $d < d_{\text{spc}}$ . This is more important in a realistic three-dimensional case, where the bandwidths are wider and the band gaps are narrower. We note that Ga edge states also appear in the main band gap for  $d > d_{\text{spc}}$ , and are identified as atomic  $4s$  states, reminiscent of  $1s$ -like edge states for the hydrogenated case. In either Ge or Ga cases, electrons are filled up to the edge states, and again the detail of the filling is dependent on the number of adatom chemical bonds.

### III. SEMICONDUCTING CHAINS WITH GE ADATOMS ON SI (100)

Semiconducting adatom chains are obtained by either group IV adatoms with two chemical bonds each, or group

III adatoms with a chemical bond each, to substrate atoms. A tight-binding view explains this in Fig. 5: (a) group IV and (b) group III adatoms, respectively. In Fig. 5(a), an adatom forms four  $sp^3$ -hybrid orbitals and is ready for chemical bonding to substrate atoms. When two  $sp^3$  orbitals meet, they form bonding and antibonding orbitals separated by double the covalent energy,<sup>5</sup> typically on the order of several eV. The remaining two dangling  $sp^3$  orbitals will rehybridize and form an  $sp$  orbital and a  $p$  orbital.<sup>5,13-15</sup> If these adatoms are arranged periodically, they form adatom bands. The  $sp$  orbital forms a valence band and the  $p$  orbital forms a conduction band. Since two additional electrons are provided from substrate atoms, we accommodate six electrons in total per unit cell. Thus, two bonding orbitals are filled and create two chemical (covalent) bonds, and the adatom valence band is fully filled, resulting in a semiconducting adatom structure.

In Fig. 5(b), the discussion runs parallel to the above. The difference is that in rehybridization, we now have two  $sp$  orbitals and two  $p$  orbitals, and one of the two  $sp$  orbitals is used for chemical bonding to a substrate atom. Two  $p$  orbitals form two conduction bands corresponding to  $\sigma$  and  $\pi$  configurations, while the other  $sp$  orbital forms a valence band. Including an electron from the substrate atom, we now have four electrons per unit cell and they fully occupy the adatom valence band as well as a bonding orbital (covalent bond), resulting again in a semiconductor.

Ge adatom structures on the Si (100) unreconstructed surface with two dangling bonds in an inset of Fig. 6 are a good example for a semiconducting chain achieving electronic isolation. Unused Si dangling bonds are hydrogenated to eliminate unwanted surface states. The ideal tetrahedral angles are assumed everywhere. This structure may not be unrealistic considering that Si and Ge are not significantly different in size, although no geometrical optimization has been performed. There are two types of adatom chains with the same lattice spacing of 3.84 Å,  $\sigma$  and  $\pi$  chains, depending on the dangling  $sp^3$ -orbitals arrangement. No rehybridization is assumed for dangling bonds in the figure for clarity, but in fact resultant adatom bands are not influenced by whether dangling bonds are rehybridized or not, or mathematically the choice of the bases.

Taking into account the charge-transfer effects among atoms up the second-nearest neighbors (Appendix B), we obtain adatom band structures in Fig. 6. The  $\sigma$  chain has a conduction-band minimum and a valence-band maximum both at  $X$ , typical to one-dimensional  $s$ - $p$  bands, while the  $\pi$  chain has a conduction-band minimum at  $\Gamma$  and a valence-band maximum at  $X$ , because of two independent  $\pi$  bands involved. The band widths are much wider than the Si bulk band gap (1.1 eV), and we expect that there would be a significant overlap between adatom and bulk Si bands. The situation is more serious in the  $\pi$  chain since the adatom band gap is as wide as 4 eV, so that at least either the conduction band or the valence band will have an entire overlap with the bulk bands.

The overlap does not immediately mean poor isolation. Surface and bulk states may be able to exist independently. This is at least not contradictory to the experimental findings. In fact, a Si (111) substrate was studied using scanning tunneling microscopy, and a normalized conductance plot as a

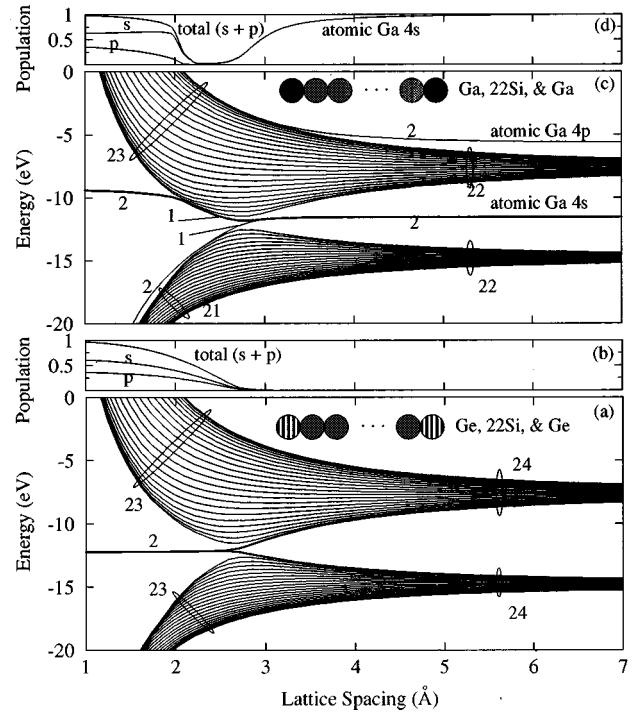


FIG. 4. Electronic states of Si chains as a function of lattice spacing: (a) energy levels and (b) edge population for states with thick line with two Ge adatoms; (c) and (d) the same plots with two Ga adatoms.

function of voltage, known to correspond to the density of states, showed five peaks, four attributed to surface states and one to bulk states.<sup>16</sup> These peak positions were consistent with those of uncoupled, unperturbed surface and bulk states.<sup>16</sup> We may argue that the coupling between these states was so weak that no significant modulation in peak positions occurred, although the experiment did not directly detect electronic isolation in the context of device applications.

Adatoms are slightly depleted ( $z_0$ ) by  $-0.0124e$  and  $-0.00626e$  ( $e$  the unit charge) and the entire adatom bands are shifted by  $-0.754$  and  $-0.0552$  eV in the  $\sigma$  and  $\pi$  chains, respectively. Both chains are positively charged, and the Fermi energy is slightly below the valence-band maximum, resulting in unintentional  $p$  doping. This simply reflects that the  $4p$  levels in Ge are slightly shallower than the  $3p$  levels in the Si (the same relation for the  $sp^3$ -hybrid levels), so that electrons tend to flow from the Ge adatoms to the Si substrate atoms. In fact, in the  $\pi$  chain, the nearest and second-nearest neighbors (both Si) are accumulated slightly. In the  $\sigma$  chain, the nearest neighbors (Si) are depleted, while the second-nearest neighbors (H) are accumulated. This is because the  $1s$  level in H is deeper than the relevant  $p$  levels in Si or Ge so that H atoms tend to absorb electrons from neighbors more efficiently. Since the  $2p$  levels in C are deeper than the  $3p$  levels in Si, the electron flow is opposite, from the Si substrate atoms to the C adatoms. Thus, C adatom chains will be unintentionally  $n$  doped. When the conditions for a semiconductor are not satisfied, adatom structures are expected to be metallic, as long as the Peierls transition or Mott transition<sup>17</sup> are irrelevant. For different adatoms, these transitions are not likely to occur since adatom structures are unintentionally doped through charge

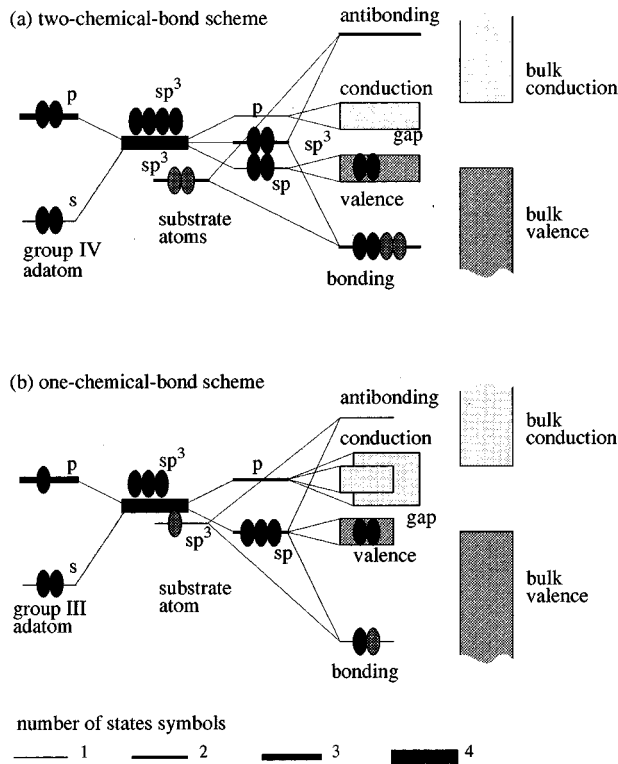


FIG. 5. Tight-binding view for semiconducting adatom chains in the chemical-bonding scheme: (a) group IV adatom with two chemical bonds and (b) group III adatom with one chemical bond.

transfer as discussed above, and the electron filling is almost always off the exact full or half.

#### IV. SUMMARY AND DISCUSSION

In the chemical bonding scheme, the electronic isolation between the adatom and substrate systems is achieved through the creation of adatom surface states localizing at the surface. The surface states exist at the dangling bonds on an  $s$ - $p$  crossing substrate such as Si, Ge, or GaAs. The isolation is better if the adatoms are electronically similar to the substrate atoms. We can eliminate or create such surface states by hydrogenation on  $s$ - $p$  crossing or uncrossing substrates, respectively. Group IV adatoms with two chemical bonds each, or group III adatoms with one chemical bond each, can form semiconducting structures. As an example for a semiconducting adatom chain with electronic isolation,  $\sigma$  and  $\pi$  chains with Ge adatoms on Si (100) are studied, and unintentional  $p$  doping is pointed out.

We need to examine practical effects on the existence of the surface states. First, an adatom may not sit directly on a substrate atom in many situations. One may model this by using two parallel chains representing a substrate with an adatom placed somewhere at each end, for example. The decay of the wave function is again a one-dimensional phenomenon, and is described as a mixture of symmetric and antisymmetric bases in each unit cell. Although the bases themselves are modified from those of the single-chain modeling, neither of them is eliminated and therefore, the effects can be absorbed in the redefinition of tight-binding parameters: the existence conditions remain unchanged. Second,

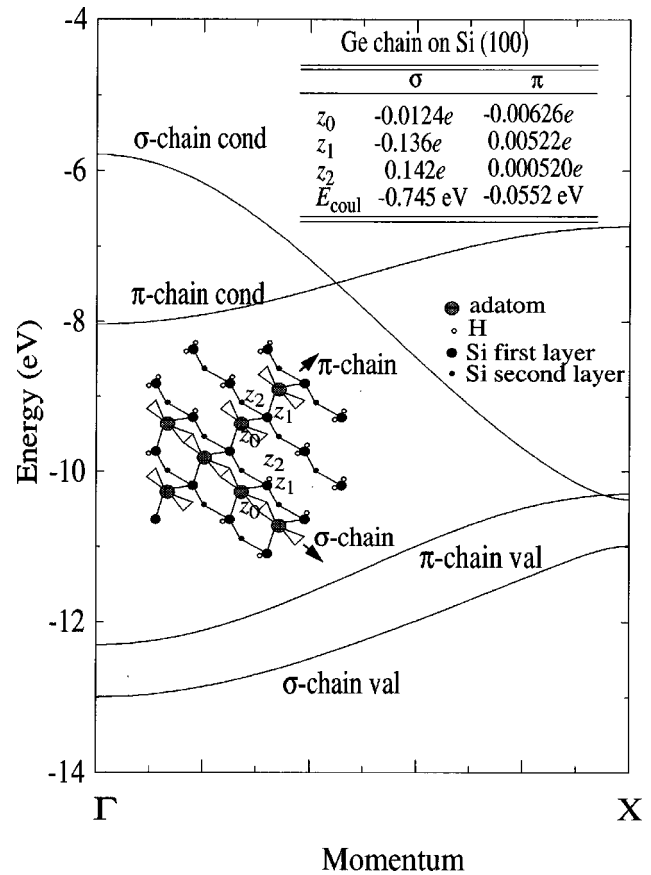


FIG. 6. Band structures for  $\sigma$  and  $\pi$  chains with Ge adatoms on hydrogenated Si (100) surface and transferred charges.

there are many different surfaces for a given crystal, but the existence does not depend on the surface orientation. As long as the substrate is  $s$ - $p$  crossing, the surface states exist on all the substrate surfaces: the substrate *bulk* properties determine the existence of the surface states. In fact, we have observed this kind of robustness in an asymmetric chain, or chains with different kinds of adatoms, where the existence of the surface states is quite insensitive to the substrate chain structure or the adatom species: only whether the bulk substrate is  $s$ - $p$  crossing or not matters. All the quantitative results such as the decay length of the wave function or the edge-state energies do sensitively depend on the adatom positions, the adatom species, or the substrate surface orientation.

In Sec. III, a tight-binding view is developed to consider whether a given adatom structure is semiconducting or not. This is also insensitive to the details of the adatom positions.<sup>18</sup> The crucial information is how many adatoms and dangling bonds there are per unit cell, and as long as the numbers do not change, the electron filling remains the same in the adatom bands and the same criteria apply. Since a different substrate surface has generally a different number of dangling bonds per unit cell, the *surface* changes the electronic properties of adatom chains, in sharp contrast to the above existence conditions. The details of the adatom bands as well as other quantitative results do depend on the exact adatom positions.

In the chemical bonding scheme, we cannot define intrinsic properties of an adatom chain. The existence of the surface modes depends on the bulk properties of the substrate,

and the electron filling of the adatom bands depends on the surface properties of the substrate. Adatom properties have to be considered for the unified adatom and substrate systems.

### ACKNOWLEDGMENTS

T.Y. gratefully acknowledges Dr. M. Meyyappan for fruitful discussions and continuous encouragement during the course of this work, and is thankful to Dr. T.R. Govindan for advice and encouragement.

### APPENDIX A: *Ab Initio* CALCULATION OF BINDING ENERGY

Our preliminary model for hydrogenated Si (111) is  $\text{Si}_6\text{H}_{12}$ , which is a six-membered Si ring with all of the dangling bonds tied off with H atoms. This cluster has  $D_{3d}$  symmetry and represents having three surface Si atoms and three second-layer Si atoms. We optimize the geometry at the second-order Moller-Plesset<sup>19</sup> (MP2) level of theory using the 6-311G\* and 6-311+G\* basis sets.<sup>20</sup> The diffuse functions in the 6-311+G\* basis set make almost no difference in the geometry. Mg is added along the threefold axis and the geometry of the entire  $\text{Si}_6\text{H}_{12}\text{Mg}$  is fully optimized at the MP2 level. The  $\text{Si}_6\text{H}_{12}$  geometry is virtually unchanged by the addition of the Mg, but they show a discrepancy of around 20% in the binding energy. Neither of these two basis sets is expected to yield an accurate Mg binding energy without some cancellation of errors for this weakly bound system. Recently Two and Pan<sup>21</sup> suggested that bond functions were a very cost effective way to compute accurate bond energies for weakly bound systems, provided the results were corrected for basis-set superposition error. Our recent results<sup>22</sup> support this observation and the addition of bond functions is the approach that we use in this work. The bond function set consists of three sp functions with exponents of 0.9, 0.3, and 0.1, two *d* functions (0.6 and 0.2) and an *f* function (0.3). We note in passing that we also tried density-functional theory (DFT), but the Mg interaction energy was very small since DFT is unable to accurately describe the van der Waals interaction. The DFT calculations, like the MP2 calculations, were performed using GAUSSIAN 94.<sup>23</sup>

On the basis of the above calibration calculation, we have optimized our  $\text{Si}_{13}\text{H}_{22}$  model as in Fig. 1, at the MP2 level using the 6-311G\* basis set with the bond functions. The height of the Mg adatom above the surface is optimized at the MP2 level using the 6-311G\* basis set with bond functions. The  $\text{Si}_{13}\text{H}_{22}$  cluster geometry is frozen to be that of the free cluster, which is consistent with the full geometry optimizations of the smaller cluster, where the cluster geometry was essentially unchanged by the presence of the Mg adatom.

### APPENDIX B: SELF-CONSISTENT TIGHT-BINDING METHOD

Adatoms are denoted by 0, the nearest neighbors by 1, and the second-nearest neighbors by 2 in a unit cell, where last two belong to the substrate. There are six unknowns,  $\epsilon_0$ ,  $\epsilon_1$ ,  $\epsilon_2$ ,  $z_0$ ,  $z_1$ , and  $z_2$ , where  $\epsilon_i$ 's are diagonal elements and  $z_i$ 's are net charges for atom *i* after self-consistent charge distribution. Original diagonal elements  $\epsilon_i^{\text{orig}}$ 's, equivalent to atomic term values,<sup>5</sup> are modified to  $\epsilon_i$ 's because of  $z_i$ 's due to the Coulomb interaction. In turn,  $z_i$ 's reflect wavefunction amplitudes and have to be determined self-consistently by  $\epsilon_1$ 's and  $V_{ij}$ 's, off-diagonal elements between atoms *i* and *j*. Using a bond-orbital approximation<sup>5</sup> and appropriate linearization,<sup>13</sup> we express this self-consistency by

$$\epsilon_i = \epsilon_i^{\text{orig}} + c_{i0}z_0 + c_{i1}z_1 + c_{i2}z_2 \quad (i=0, 1, \& 2),$$

$$z_0 = (\epsilon_1 - \epsilon_0)/V_{01},$$

$$z_1 = (\epsilon_0 - \epsilon_1)/(2V_{01}) + (\epsilon_2 - \epsilon_1)/(2V_{12}),$$

$$z_2 = (\epsilon_1 - \epsilon_2)/(2V_{12}).$$

$c_{ij}$  represents the Coulomb interaction for atom *i* due to charge  $z_j$  reflecting their distance, and this includes the intra-atomic (charging) and interatomic (Madelung) interactions. Necessary tight-binding parameters for H are taken from Ref. 24 and those for Ge and Si from Ref. 13. Once all the constants are determined, numerical solution is easy after a routine matrix inversion.

\*Electronic address: yamada@nas.nasa.gov

<sup>1</sup>H.-S. Wong and Y. Taur, Tech. Dig., Int. Electron Devices Meet. **1993**, 705.

<sup>2</sup>J.-R. Zhou and D. K. Ferry, IEEE Comput. Sci. Eng. **2**, 30 (1995).

<sup>3</sup>J. R. Tucker and T.-C. Shen, Solid-State Electron. **42**, 1061 (1998).

<sup>4</sup>For example, D. M. Eigler and E. K. Schweizer, Nature (London) **344**, 524 (1990); I.-W. Lyo and Ph. Avouris, Science **253**, 173 (1991); H. J. Hamin, S. Chiang, H. Birk, P. H. Guenther, and D. Ruger, J. Vac. Sci. Technol. B **9**, 1398 (1991); M. F. Crommie, C. P. Lutz, and D. M. Eigler, Science **262**, 218 (1993); Ph. Ebert, M. G. Lagally, and K. Urban, Phys. Rev. Lett. **70**, 1473 (1993); Ph. Avouris, I.-W. Lyo, and Y. Hasegawa, J. Vac. Sci. Technol. A **11**, 1725 (1993); H. Uchida, D. Huang, F. Grey, and M. Aono, Phys. Rev. Lett. **70**, 1437 (1993); C. T. Salling and M. G. Lagally, Surf. Sci. **265**, 502 (1994); A. Yazdani, D. M. Ei-

gler, and N. D. Lang, Science **272**, 1921 (1996).

<sup>5</sup>W. A. Harrison, *Electronic Structure and Properties of Solids* (Freeman, San Francisco, 1980).

<sup>6</sup>W. A. Harrison, Surf. Sci. **299/300**, 298 (1994); Phys. Rev. B **24**, 5835 (1981).

<sup>7</sup>T. Yamada, J. Vac. Sci. Technol. B **15**, 1019 (1997); T. Yamada, Y. Yamamoto, and W. A. Harrison, *ibid.* **14**, 1243 (1996).

<sup>8</sup>T. Yamada, J. Vac. Sci. Technol. A **16**, 1403 (1998).

<sup>9</sup>Ph. Avouris, R. E. Walkup, A. R. Rossi, H. C. Akpati, P. Nordlander, T.-C. Shen, G. C. Abeln, and J. W. Lyding, Surf. Sci. **363**, 368 (1996).

<sup>10</sup>W. Shockley, *Electrons and Holes in Semiconductors* (Van Nostrand, Princeton, 1950).

<sup>11</sup>W. Shockley, Phys. Rev. **56**, 317 (1939).

<sup>12</sup>J. C. Slater, *Quantum Theory of Matter* (McGraw-Hill, New York, 1968).

- <sup>13</sup>W. A. Harrison and J. E. Klepeis, *Phys. Rev. B* **37**, 864 (1988); J. E. Klepeis and W. A. Harrison, *J. Vac. Sci. Technol. B* **6**, 1315 (1988).
- <sup>14</sup>J. E. Klepeis and W. A. Harrison, *Phys. Rev. B* **40**, 5810 (1989).
- <sup>15</sup>The same physics can be described differently, without going through the hybridization and rehybridization. An adatom is assumed to form three  $sp^2$  orbitals and a  $p$  orbital, like a C atom in graphite. Then, two  $sp^2$  orbitals are used for the substrate bonding, the remaining one  $sp^2$  orbital for a valence band, and the  $p$  orbital for a conduction band. Two views give the same qualitative adatom bands, and the only difference is that the valence band originates from either  $sp$  (text) or  $sp^2$  (here), respectively. The real system will be somewhat between these two, and a rigorous distinction is important when experimental data are available.
- <sup>16</sup>J. A. Stroschio, R. M. Feenstra, and A. P. Fein, *Phys. Rev. Lett.* **57**, 2579 (1987).
- <sup>17</sup>R. Peierls, *Quantum Theory of Solids* (Oxford University, Oxford, 1955); N. F. Mott and E. A. Davis, *Electronic Processes in Non-crystalline Materials* (Clarendon, Oxford, 1979).
- <sup>18</sup>K. C. Pandey, *Phys. Rev. Lett.* **47**, 1913 (1981); **49**, 223 (1982); S. Watanabe, Y. A. Ono, T. Hashizume, and Y. Wada, *Phys. Rev. B* **54**, 17 308 (1996).
- <sup>19</sup>J. A. Pople, J. S. Binkley, and R. Seeger, *Int. J. Quantum Chem., Symp.* **10**, 1 (1976).
- <sup>20</sup>M. J. Frisch, J. A. Pople, and J. S. Binkley, *J. Chem. Phys.* **80**, 3265 (1984), and references therein.
- <sup>21</sup>F.-M. Tao and Y.-K. Pan, *J. Chem. Phys.* **97**, 4989 (1992).
- <sup>22</sup>H. Partridge and C. W. Bauschlicher, Jr., *Mol. Phys.* **96**, 705 (1999).
- <sup>23</sup>GAUSSIAN 94, Revision D.1., M. J. Frisch, G. W. Trucks, H. B. Schlegel, P. M. W. Gill, B. G. Johnson, M. A. Robb, J. R. Chessexman, T. Keith, G. A. Petersson, J. A. Montgomery, K. Raghavachari, M. A. Al-Laham, V. G. Zakrzewski, J. V. Ortiz, J. B. Foresman, J. Cioslowski, B. B. Stefanov, A. Nanayakkara, M. Challacombe, C. Y. Peng, P. Y. Ayala, W. Chen, M. W. Wong, J. L. Andres, E. S. Replogle, R. Gomperts, R. L. Martin, D. J. Fox, J. S. Binkley, D. J. Defrees, J. Baker, J. P. Stewart, M. Head-Gordon, C. Gonzalez, and J. A. Pople (Gaussian, Inc., Pittsburgh, 1995).
- <sup>24</sup>D. C. Allan and E. J. Mele, *Phys. Rev. B* **31**, 5565 (1985).